

Article

## Release of Potassium Ion and Calcium Ion from Phosphorylcholine Group Bearing Hydrogels

Hanna R. Aucoin<sup>1,2</sup>, A. Nolan Wilson<sup>1,2</sup>, Ann M. Wilson<sup>3,4</sup>, Kazuhiko Ishihara<sup>5</sup> and Anthony Guiseppi-Elie<sup>1,2,4,\*</sup>

<sup>1</sup> Center for Bioelectronics, Biosensors and Biochips (C3B), Clemson University Advanced Materials Center, 100 Technology Drive, Anderson, SC 29625, USA;

E-Mails: haucoin@g.clemson.edu (H.R.A.); anwilso@clemson.edu (A.N.W.)

<sup>2</sup> Department of Chemical and Biomolecular Engineering, 132 Earle Hall, Clemson University, Clemson, SC 29634, USA

<sup>3</sup> Department of Chemistry, University of the West Indies, St. Augustine, Trinidad and Tobago; E-Mail: ann.wilson@sta.uwi.edu

<sup>4</sup> ABTECH Scientific, Inc., Biotechnology Research Park, 800 East Leigh Street, Richmond, VA 23219, USA; E-Mail: amwilson@abtechsci.com

<sup>5</sup> Department of Materials Engineering and Department of Bioengineering, School of Engineering, The University of Tokyo, 7-3-1, Hongo, Bunkyo-ku, Tokyo 113-8656, Japan; E-Mail: ishihara@mpc.t.u-tokyo.ac.jp

\* Author to whom correspondence should be addressed; E-Mail: guiseppi@clemson.edu; Tel.: +1-864-656-1712; Fax: +1-864-656-1713.

Received: 28 September 2013; in revised form: 17 October 2013 / Accepted: 25 October 2013 /

Published: 11 November 2013

---

**Abstract:** In an attempt to recreate the microenvironment necessary for directed hematopoietic stem cell differentiation, control over the amount of ions available to the cells is necessary. The release of potassium ion and calcium ion via the control of cross-linking density of a poly(2-hydroxyethyl methacrylate) (pHEMA)-based hydrogel containing 1 mol % 2-methacryloyloxyethyl phosphorylcholine (MPC) and 5 mol % oligo(ethylene glycol) (400) monomethacrylate [OEG(400)MA] was investigated. Tetra(ethylene glycol) diacrylate (TEGDA), the cross-linker, was varied over the range of 1–12 mol %. Hydrogel discs ( $\phi = 4.5$  mm and  $h = 2.0$  mm) were formed by UV polymerization within silicone isolators to contain 1.0 M CaCl<sub>2</sub> and 0.1 M KCl, respectively. Isothermal release profiles, were measured at 37 °C in 4-(2-hydroxyethyl)-1-piperazineethanesulfonic acid sodium salt (HEPES) buffer using either calcium ion or potassium ion selective electrodes (ISE). The resulting release

profiles were found to be independent of cross-linking density. Average ( $n = 3$ ) release profiles were fit to five different release models with the Korsmeyer-Peppas equation, a porous media transport model, exhibiting the greatest correlation ( $R^2 > 0.95$ ). The diffusion exponent,  $n$  was calculated to be  $0.24 \pm 0.02$  and  $0.36 \pm 0.04$  for calcium ion and potassium ion respectively indicating non-Fickian diffusion. The resulting diffusion coefficients were calculated to be  $2.6 \times 10^{-6}$  and  $11.2 \times 10^{-6}$  cm<sup>2</sup>/s, which compare well to literature values of  $2.25 \times 10^{-6}$  and  $19.2 \times 10^{-6}$  cm<sup>2</sup>/s for calcium ion and potassium ion, respectively.

**Keywords:** calcium ion; potassium ion; diffusion; 2-methacryloyloxyethyl phosphorylcholine; poly(2-hydroxyethyl methacrylate); hydrogel matrix; Zwitterionic; HEMA

---

## 1. Introduction

Bioactive hydrogels have over the past decade gained traction as polymers for the abio-bio interface in indwelling bioelectronics [1], as drug delivery matrices [2,3], and as tissue scaffolds in regenerative medicine [4]. Much of this attention is because of their high biocompatibility [5], attributed partially to their ability to imbibe large amounts of water [6], to mitigate denaturing protein adsorption, and because of their stimuli responsive nature [7], attributed partially to swelling-collapsing dynamics that are dependent on environmental conditions [8–10]. Because of the importance of diffusive transport in many aspects of molecular physiology, an area currently under investigation is the design and molecular engineering of the diffusive transport properties of small molecules and ions within the hydrogel matrix as a means towards control of expressed bioactivity. Of particular importance, ion transport through hydrogels can be used within engineered scaffolds to control cell-matrix and cell-cell interactions in osteoblast cultures [11], in electro-stimulated release of bioactive compounds [12], and to maintain on-eye movement in silicone contact lenses [13]. It has been shown that diffusion in acrylate and methacrylate based hydrogels can be regulated by varying the degree of hydration [14] through the use of bi-functional monomers such as tetra(ethylene glycol) diacrylate (TEGDA) [15].

In previous work, we have reported on the permeability of hydrogel membranes to Ca<sup>++</sup> as measured by time-lag technique when the hydrogel was cast as a film that was supported on a track-etch, nano-pore membrane of a cell culture insert [14]. The porous media model was found to adequately explain the cross-link density dependence of the partition/diffusion permeability of Ca<sup>++</sup> through the hydrogel layer. Ion diffusion in hydrogels is important in the design and application of wetting and disinfection agents for soft contact lenses, in controlling ocular drug delivery and in partitioning and concentration applications. Ion partitioning and rate of diffusion are influenced by ion and hydrogel charge, the hydrodynamic radius of the ion and the hydrogel mesh size. Ion partitioning depends upon the availability of suitably sized water-filled voids in the surface of the hydrogel that serve to de-solvate the ion and adsorb it into the hydrogel mesh. Diffusion depends upon the frequency of occurrence of such water-filled voids to support hindered diffusion through the polymer mesh. Apparent diffusivities of ions within hydrogels are thus expected to be reduced relative to their values in aqueous solution due to interaction with the polymer chains including hydrodynamic drag, electrostatic drag and physical obstruction that are best represented by the Brinkman-Effective-Medium model [16].

The distribution of void sizes supposes that only voids above a critical volume, corresponding to larger than the hydrodynamic radius of the ion, will support diffusion and will thus confer the expected hydrodynamic and electrostatic drag. Voids below this critical volume are obstructions. Indeed, a complete understanding of ion transport within charged polymers, so important in bioelectronics and biofuel cells, continues to require detailed attention [17].

In addition to covalent crosslinking, hydrogels can be rendered insoluble by virtual crosslinks formed by charged main chain and/or pendant groups that are capable of electrostatic bonding to themselves and to imbibed free ions [18]. Swelling of hydrogels, driven by thermodynamics, is governed by the solvating forces involved with polymer-solvent mixing, the relaxation forces involved with the elasticity of the crosslinks, and the osmotic pressure introduced by ionic forces [19,20]. The extent of hydrogel swelling in a salt solution will depend on external and internal ion concentration, which influences the balance between the solvating and retractive forces. The distribution of ions between hydrogel and solution results in larger charge concentrations in the solution and typically result in reduced equilibrium swelling [2,21]. Hence, the higher the external concentration of ions (reduced activity of water), the lower the equilibrium swelling and a correspondingly lower apparent diffusion coefficient is expected. Additionally, the presence of and extent of ionization of zwitterionic groups of monomer such as 2-methacryloyloxyethyl phosphorylcholine (MPC) units may affect imbibed ion concentration through surface adsorption of ions [22] and through the creation of ionic domains within the hydrogel. This is vitally important as the phosphorylcholine group of MPC moiety is expected to migrate to the interface and influence protein adsorption at the hydrogel-electrolyte interface [5,23]. Also, the apparent diffusion coefficient of ions within the hydrogel may be increased, despite osmotic de-swelling, as diffusing ions move along channels created by the linking of these ion-rich voids. Previous characterizations of ionic transport through biocompatible hydrogel matrices have yet to illuminate the effect of zwitterionic moieties on the transport of ions.

In this work, cross-linked biomimetic poly(2-hydroxyethyl methacrylate) (pHEMA)-based hydrogels containing MPC units (1 mol %) and oligo(ethylene glycol) (400) monomethacrylate [OEG(400)MA] (5 mol %), added for improved biocompatibility, were studied for their influence on ion transport properties of monovalent potassium cations ( $K^+$ ) and divalent calcium cations ( $Ca^{++}$ ), respectively. To influence ion transport properties, the cross-link density was varied through a variation in the concentration of TEGDA over the range of 1–12 mol % and the release of potassium ion and calcium ion studied at 37 °C using ion sensitive electrodes (ISEs). The mol % TEGDA concentration captures a crosslinker concentration range pertinent to biosensors [24], drug release [3], and biocompatibility [25]. By studying the release of monovalent and divalent cations, it is expected that the release can serve as a surrogate and inform transport of other ionizable species.

## 2. Experimental Section

### 2.1. Reagents

Anhydrous calcium chloride ( $CaCl_2$ ) was purchased from Sigma Aldrich (Milwaukee, WI, USA). The hydrogel components; HEMA, *N*-[tris(hydroxymethyl)methyl]acrylamide (HMMA, 93%), OEG(400)MA, poly(*N*-vinyl pyrrolidone) (pNVP,  $M_w = 1.3 \times 10^6$ ), as well as the divalent cross linker,

TEGDA, and the photoinitiator 2,2-dimethoxy-2-phenylacetophenone (DMPA, 99%) were purchased from Sigma Aldrich. The MPC was prepared elsewhere as described [26]. The polymerization inhibitors hydroquinone and monomethyl ether hydroquinone were removed by passing the liquid methacrylate and acrylate-containing constituents over an inhibitor removal column. The buffer salt, 4-(2-hydroxyethyl)-1-piperazineethanesulfonic acid sodium salt (HEPES), was made to 0.1 M, pH = 7.35, and pH-adjusted by drop-wise addition of 1.0 M HCl. Deionized (MilliQ DI, Billerica, MA, USA) water was used to prepare all of the solutions.

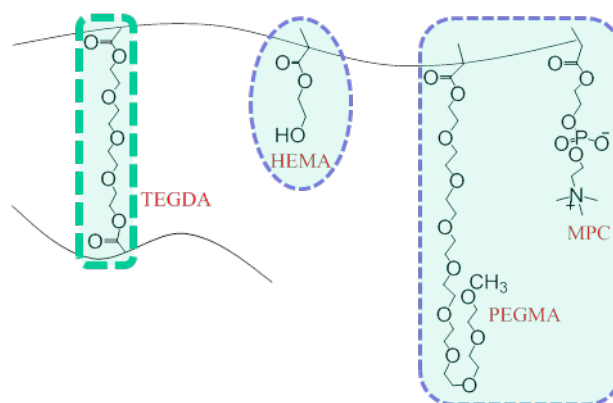
## 2.2. Preparation of Monomer Cocktail and Synthesis of Hydrogel Discs

Biocompatible, biomimetic hydrogel cocktails were prepared by combining HEMA, OEG(400)MA, HMMA, MPC, pNVP, TEGDA, DMPA, and varying the mol percent of crosslinker, TEGDA, shown in Table 1. The mixture was ultrasonicated for 5 min and subsequently sparged with nitrogen to remove dissolved air (oxygen). To increase the solubility of the monomer constituents, a 1:1 (v/v) of ethylene glycol and water was added such that the solvent was 20 vol % of the final mixture. A representation of the resulting macromolecular network structure is shown in Figure 1. Two separate sets of cocktail solutions were loaded with ionic salts. The first was loaded with anhydrous calcium chloride to a final concentration of 1.0 M within the hydrogel and the second with potassium chloride to a final concentration of 0.1 M (due to solubility limitations) within the hydrogel.

**Table 1.** Hydrogel constituents.

Constituent	Mole fraction (mol %)					
HEMA	85.0	83.0	81.0	79.0	77.0	74.0
TEGDA	1.0	3.0	5.0	7.0	9.0	12.0
OEG(400)MA	5.00	5.0	5.0	5.0	5.0	5.0
MPC	1.0	1.0	1.0	1.0	1.0	1.0

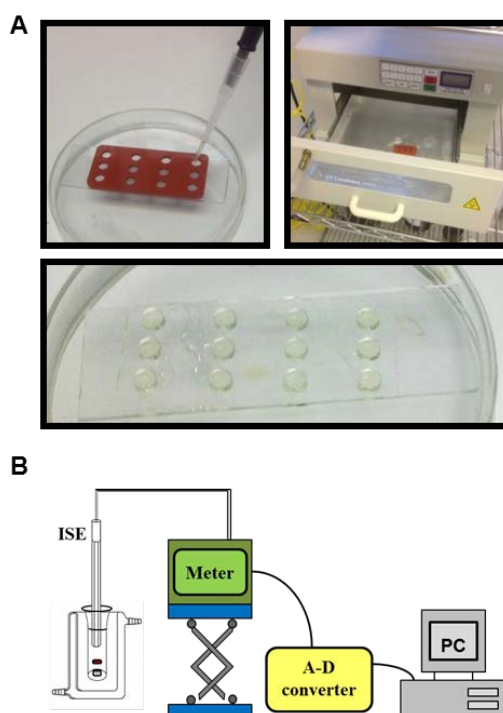
**Figure 1.** Schematic of the molecular structure and pre-polymer constituents of poly(HEMA)-based hydrogel possessing MPC, OEG(400)MA and varying crosslink density based on mole fraction of TEGDA.



To fabricate hydrogel disks, 30  $\mu$ L aliquots of each hydrogel cocktail was pipetted evenly into silicon isolators (JTR12R-2.0, Grace Biolabs, Bend, OR, USA) of thickness,  $h = 2.0$  mm and diameter  $\phi = 4.5$  mm. The mixtures were immediately placed in a UV crosslinker (CX-2000, UVP, Upland,

CA, USA) and UV irradiated at 366 nm for 5 min under an inert nitrogen atmosphere to polymerize the hydrogel disks. After polymerization, the hydrogel disks were removed from the isolator, Figure 2A. The hydrogels, preloaded with salt, were placed in individual storage vials and stored at 4 °C until use.

**Figure 2.** (A) The liquid hydrogel cocktail was loaded into silicon isolators (**top left panel**) and then polymerized using UV light (**top right panel**). The polymerized hydrogels were then removed from the isolators (**bottom panel**); and (B) Experimental set-up for measuring calcium ion and potassium ion release into HEPES buffer.



### 2.3. Release of Charged Species

Concentration of cations was measured using a calcium ion selective electrode (ISE) and potassium ion ISE, respectively. The ISE was immersed in 3 mL of HEPES buffer, the release solution, which maintained a pH of 7.4, a temperature of 37 °C, and was continuously stirred during the release. Measurements were gathered using a data acquisition device (DATAQ Instruments, Inc., Akron, OH, USA) and the accompanying software recorded the data in Excel, Figure 2B. Release was initiated by immersing the hydrogel disk into the release solution, which already contained the ISE, and the release was measured until equilibrium was reached.

The measured ISE outputs in millivolts were converted into ion concentration based on the use of measured calibration plots. Calibration ladders (Supplementary Information Figures S1 and S2) were generated for the ISE using known concentrations derived from serial dilutions of either  $\text{CaCl}_2$  or  $\text{KCl}$  prepared in 0.1 M 2-amino-2-hydroxymethyl-propane-1,3-diol (TRIS) buffer. Triplicate measures were made in ascending, descending and random order. The voltages of these known concentrations were measured to produce a calibration curve from which other millivolt values could be converted into ion concentration. The relation of concentration to millivolt is log-linear and is described by the Nernst equation:

$$E^0 - E = V = \frac{RT}{zF} \ln[M_t] \tag{1}$$

where,  $E$  is the electrode potential at nonstandard conditions,  $E^0$  is the electrode potential at standard conditions,  $V$  is the equilibrium potential measured by the ISE,  $T$  is the absolute temperature,  $F$  is Faraday’s constant,  $R$  is the ideal gas constant,  $z$  corresponds to the ion charge (e.g., for calcium ion  $z$  is +2 and for potassium ion  $z$  is +1), and  $[M_t]$  is the concentration of ions in the release solution.

After obtaining and converting the raw data, the results were fit to five models transport models, Zero-Order, First-Order, Higuchi, Hixon-Crowell Cube Root, and Korsmeyer-Peppas, using non-linear least-squared regression, Table 2. A detailed description of assumption for each model is given in the supplementary material.

**Table 2.** Transport Models.

Model	Model Equation	Equation No.	Ref.
Zero-Order	$M_0^{gel} - M_t^{gel} = k_0 t$	(2)	[25]
First-Order	$\ln\left(\frac{M_0^{gel}}{M_t^{gel}}\right) = kt$	(3)	[25]
Higuchi	$M_t^{gel} = k_H t^{1/2}$	(4)	[27]
Hixon-Crowell Cube Root	$W_0^{gel^{1/3}} - W_t^{gel^{1/3}} = \kappa t$	(5)	[28]
Korsmeyer-Peppas	$\frac{M_t^{sol}}{M_\infty^{sol}} = k_{KP} t^n$	(6)	[29]

where,  $M_0^{gel}$  is the initial concentration of cation present in the hydrogel,  $M_t^{gel}$  is the concentration of cation present in the hydrogel at time  $t$ ,  $k_0$  is the Zero-Order release constant,  $k$  is the First-Order release constant,  $k_H$  is the Higuchi dissolution constant,  $W_0^{gel}$  is the mass of the salt initially present within the hydrogel,  $W_t^{gel}$  is the mass of the salt at time  $t$ , and  $\kappa$  is a constant incorporating the relationship between the surface area and the volume of the salt molecule,  $M_t^{sol}$  is the concentration of the salt in the release solution at time  $t$ ,  $M_\infty^{sol}$  is the equilibrium concentration of the salt in the release solution,  $k_{KP}$  is the Korsmeyer-Peppas release rate constant, and  $n$  is the diffusional exponent.

The diffusional exponent,  $n$ , in the Korsmeyer-Peppas model, informs the mechanism of diffusional release. Table 3 shows the possible diffusional exponents and corresponding release mechanisms for a cylindrically shaped sample. In determining the value of  $n$ , the data fitting was performed on the portion of the release curve where  $\frac{M_t^{sol}}{M_\infty^{sol}} < 0.6$ .

**Table 3.** Diffusional exponent and diffusional release mechanisms for a cylindrical sample [29].

Diffusional exponent, $n$	Drug release mechanism	Rate as a function of time
$\geq 0.45$	Fickian diffusion	$t^{-0.5}$
$0.45 < n < 0.89$	Anomalous transport	$t^{n-1}$
0.89	Case-II transport	Zero-Order release
$n > 0.89$	Super case-II transport	$t^{n-1}$

The effective diffusivity is related to the release of ions in solution as follows:

$$\frac{M_t^{\text{sol}}}{M_{\infty}^{\text{sol}}} = 4 \left( \frac{D_{\text{eff}} t}{\pi L^2} \right)^n \quad (7)$$

where  $D_{\text{eff}}$  is the effective diffusivity,  $L$  is the diameter of the hydrogel disc, and  $n$  is the diffusional exponent. From Equation 7, the Korsmeyer-Peppas constant can be related to the effective diffusivity.

$$D_{\text{eff}} = \pi L^2 \left( \frac{k_{\text{KP}}}{4} \right)^{\frac{1}{n}} \quad (8)$$

### 3. Results and Analysis

#### 3.1. Release Profiles of Ions

Figure 3 shows the release profiles of calcium ion and potassium ion from hydrogels into TRIS buffer at 37 °C and pH 7.4. The concentration of ions in the release solution at a given time ( $M_t$ ) was normalized to the equilibrium ion concentration in the release solution ( $M_{\infty}$ ) and plotted as a function of time for each crosslink density, 1, 3, 5, 7 and 9 mol % TEGDA. Normalization was used to eliminate release dependence on the initial ion concentration in the gel. Figure 3A,B show the release profiles of potassium ion and calcium ion, respectively, for each crosslinking density. The averaged release profile for each of calcium ion and potassium ion is shown in Figure 3C.

**Figure 3.** (A) Potassium ion and (B) Calcium ion release profiles for varying concentration of TEGDA during preparation of the hydrogels; and (C) Average release profiles for both ionic species.

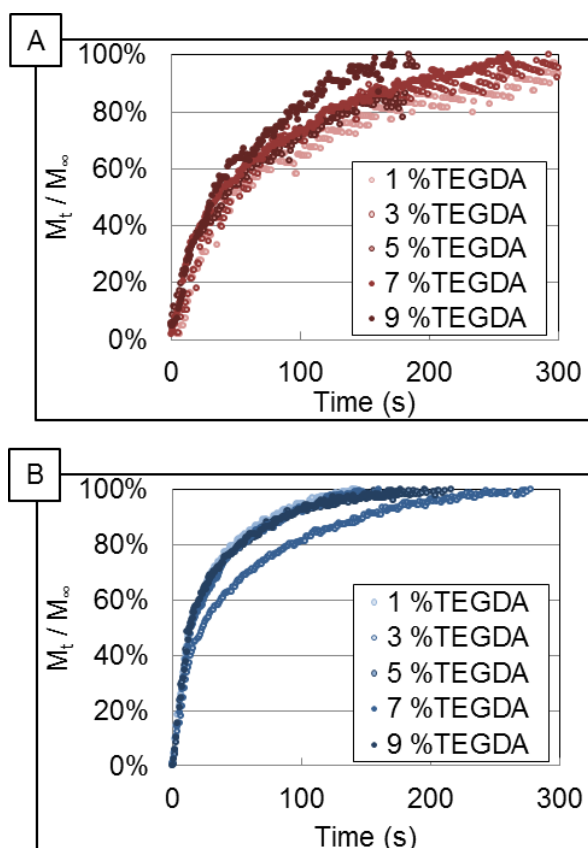
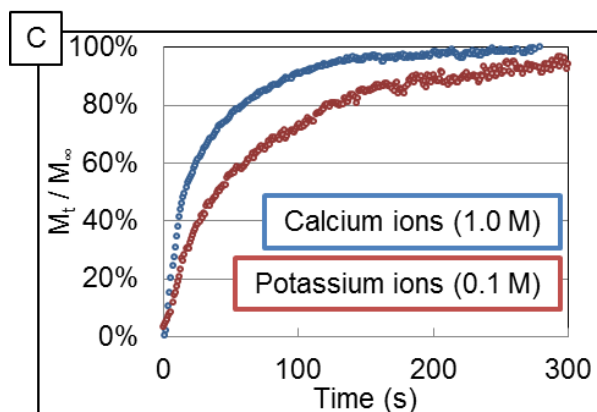


Figure 3. Cont.



### 3.2. Data Analysis

Nonlinear least squares fits were performed for all five transport models for each of the various cross-link densities. The resulting  $R$ -squared values of the fits for calcium ion release and potassium ion release are shown in Table 4. The First-Order and Korsmeyer-Peppas model both demonstrated high correlation to the experimental data; however, Korsmeyer-Peppas was selected for further analysis as additional mechanistic information can be interpreted from the  $n$  parameter and  $k_{KP}$  can be directly related to effective diffusivity.

**Table 4.**  $R$ -squared values for non-linear least square fits of calcium ion release profiles to Equations (2)–(6) for varying crosslink density and the overall average  $R$ -squared value for each equation.

mol % Crosslinker	Zero-Order	First-Order	Higuchi	Hixson-Crowell	Korsmeyer-Peppas
<b>Potassium ion</b>					
1% TEGDA	−0.63	0.89	0.65	−0.60	0.87
3% TEGDA	−0.34	0.91	0.75	−0.32	0.88
5% TEGDA	−0.07	0.83	0.76	−0.05	0.89
7% TEGDA	−0.10	0.91	0.87	−0.04	0.96
9% TEGDA	0.02	0.93	0.86	0.05	0.94
<b>Calcium ion</b>					
1% TEGDA	−2.01	0.94	0.28	−1.99	0.90
3% TEGDA	−1.95	0.91	0.34	−1.93	0.92
5% TEGDA	−2.32	0.91	0.17	−2.29	0.88
7% TEGDA	−1.21	0.93	0.56	−1.19	0.92
9% TEGDA	−1.35	0.90	0.50	−1.33	0.91

### 3.3. Korsmeyer-Peppas Fit Parameters

The variables involved in Equation (8),  $k_{KP}$ ,  $D_{eff}$  and  $n$ , were calculated for potassium ion and calcium ion release across varying crosslink densities as shown in Table 5 and plotted in Supplementary Information Figures S3–S5, Tables S3–S5.

**Table 5.** Average Korsmeyer-Peppas constants, diffusion coefficients, and effective diffusivity values obtained using the Korsmeyer-Peppas model for calcium ion and potassium ion. Error is reported for  $n = 3$  unless otherwise indicated.

Model parameter	Ion Type	% TEGDA				
		1.0	3.0	5.0	7.0	9.0
$K_{KP}$	Calcium ion	$0.30 \pm 0.09$	$0.25 \pm 0.13$	$0.31 \pm 0.08$	$0.24 \pm 0.09$	$0.26 \pm 0.12$
	Potassium ion	$0.15 \pm 0.84^\dagger$	$0.14 \pm 0.11^\dagger$	$0.30 \pm 0.32$	$0.14 \pm 0.02$	$0.12 \pm 0.08$
$n$	Calcium ion	$0.24 \pm 0.11$	$0.25 \pm 0.12$	$0.24 \pm 0.07$	$0.27 \pm 0.04$	$0.26 \pm 0.05$
	Potassium ion	$0.32 \pm 0.90^\dagger$	$0.33 \pm 0.16^\dagger$	$0.39 \pm 0.36$	$0.35 \pm 0.03$	$0.38 \pm 0.18$
$D_{eff}$	Calcium ion	$3.2 \pm 10 \times 10^{-6}$	$2.2 \pm 5.9 \times 10^{-6}$	$1.4 \pm 2.7 \times 10^{-6}$	$3.4 \pm 4.4 \times 10^{-6}$	$3.0 \pm 2.0 \times 10^{-6}$
	Potassium ion	$3.5 \pm 31 \times 10^{-6}^\dagger$	$5.1 \pm 14 \times 10^{-6}^\dagger$	$17 \pm 34 \times 10^{-6}$	$8.6 \pm 4.2 \times 10^{-6}$	$17 \pm 37 \times 10^{-6}$

Note:  $^\dagger n = 2$ .

#### 4. Discussion

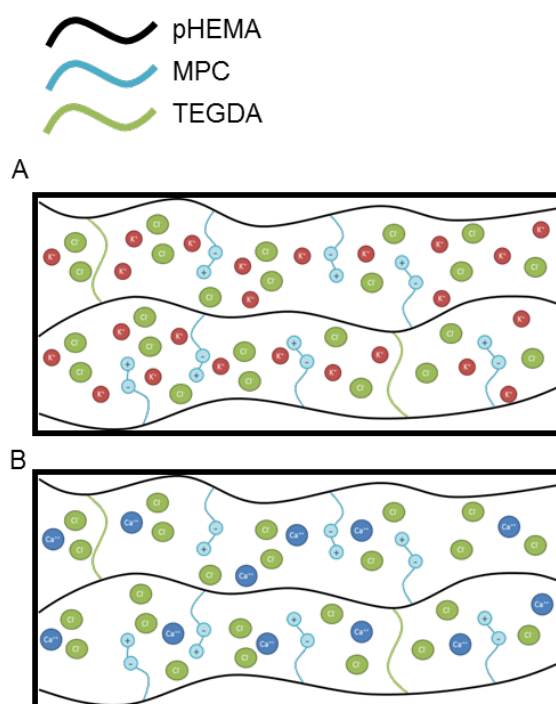
The complexities of ion transport through a hydrogel matrix bearing zwitterionic groups are schematically illustrated in Figure 4. Two phenomenological effects can contribute to the transport of ions out of a hydrogel matrix: diffusion due to concentration gradients and electromigration due to charge density gradients. Diffusion of small, uncharged molecules through neutral hydrogels has been shown to be attenuated by increased crosslinking density which changes the free volume available for transport and can be modeled using porous media or free volume models [15]. Systems such as these have been thoroughly characterized in the literature and reveal a clear linear dependence of crosslink density on crosslinker feed composition [30]. This is particularly true for the low crosslinker compositions used in this work. Also, the calculated mesh size follows the expected asymptotic decrease with increasing crosslinker composition predicted by swelling theory [8]. According to these models, the diffusion coefficient,  $D$ , of a solute depends on both properties of the solute and the local properties of the polymer hydrogel. This is often expressed relative to the reference diffusion in pure solvent,  $D_0$ , the polymer mesh size,  $\xi$ , the hydrodynamic radius of the solute,  $r_s$ , polymer fraction in the swollen state,  $v_{2,s}$ , polymer-solute interactions, crosslink density and polymer chain mobility. Thus, a general form for such a model is given by

$$\frac{D}{D_0} = f(\xi, r_s, v_{2,s}) \quad (9)$$

For hydrogels, when the polymer mesh size or characteristic length,  $\xi \gg r_s$ , the hydrodynamic radius of the diffusing solute, then interactions between the solute and the polymer segments/pendants are minimized and the diffusion coefficient may be related to the porosity and tortuosity of the porous structure; for which a porous media model is appropriate [14]. However, when the characteristic length approaches the size of the solute molecule, interactions between the solute and the hydrogel structure become important. One approach to empirically investigate this effect is to gradually change the crosslink density. The transport of charged molecules or ions is a more complex process as the state of water (free or bound), ion partitioning, the hydrodynamic radii of the cations and/or counter anions and electrostatic shielding effects can each contribute significantly to the transport process as shown by Hamilton *et al.* [31]. While much work has been done in this area the effects of electrostatic interactions

and the role of charge loading is still lacking for transport of ions through hydrogels bearing zwitterionic groups. These hydrogel matrices could engender further complexity as one-to-one (one ion to one binding site on the hydrogel matrix) or one-to-two (one ion to two binding sites on the hydrogel matrix) electrostatic interactions may perturb transport properties through retention of ions due to ion binding or through virtual crosslinks thereby increasing the effective crosslink density. Such potential electrostatic one-to-one and one-to-two interactions are illustrated schematically in Figure 4A,B, for potassium ion and calcium ion, respectively. Additionally, charge loading could play a role in how the ions are released from the hydrogel by creating cage effects and large potential gradients between the hydrogel and the release solution. It should be noted that partitioning effects are not considered in this discussion as it has been shown that the partition coefficient has little effect on cation transport [31].

**Figure 4.** Schematic illustration of charge distribution and electrostatic interactions between (A) potassium ion and (B) calcium ion and PC in MPC containing hydrogel.



Moreover, inner-salt formation of the phosphorylcholine groups of the MPC units has been shown to occur [32]. Indeed, the conformation of the poly(MPC) did not change when immersed in salt solutions [33]. Instead of the direct interaction between ions and PC moieties of MPC units, it is likely the increased activity of water that accompanies the addition of salts that influences the diffusion behaviour through the hydrogel matrix.

The release profiles of calcium ion and potassium ion shown in Figure 3A,B were found to be independent of crosslink density over the range of TEGDA concentration studied. This is in sharp contrast to the observation of a cross-linker dependence when calcium ions are made to partition into voids and transport by diffusion across similarly comprised hydrogels within a two-compartment cell [14]. The normalized composite release profiles, Figure 3C, indicate that the release profile is dependent only upon the identity of the cation. Further analysis using the Korsmeyer-Peppas model supported the cross-linker independent nature of the release profiles as the fitting parameters of the

model remained constant over various cross-link densities. Because no correlation was observed between the cross-link density and the apparent diffusion coefficient, the average values of transport parameters for each ion were directly compared. The average effective diffusivity of potassium ion and calcium ion were  $(11.2 \pm 6.2) \times 10^{-6}$  and  $(2.6 \pm 1.2) \times 10^{-6}$  cm<sup>2</sup>/s, respectively ( $p = 0.011$ ). These values indicate that potassium ions diffuse five times faster than calcium ions. However, the observed release profiles of potassium ion and calcium ion are reversed given these values as calcium ion is released more rapidly from the hydrogel than potassium ion. This cannot be explained by consideration of hydrodynamic radii as these values are 2.12 and 2.76 Å for potassium ion and calcium ion, respectively. Similarly, these observations cannot be explained by consideration of the charge densities (charge/hydrodynamic volume) as these are quite similar, being 0.0251 and 0.0227 Å<sup>-3</sup> for potassium ion and calcium ion, respectively. This apparent contradiction may have its explanation in the value of the  $n$  parameter of the Korsmeyer-Peppas model. The average value of  $n$  for potassium ion and calcium ion was determined to be  $0.36 \pm 0.05$  and to be  $0.24 \pm 0.02$ , respectively ( $p = 0.0001$ ). Both of these average  $n$  values are less than 0.5 indicating that the transport mechanism of potassium ion and calcium ion is non-Fickian. Electrostatic interactions such as ion-pair binding, virtual cross-linking and/or electromigration are potential sources of this non-Fickian behaviour. The total charge per unit volume within the hydrogels was initially 9.7 and 193.0 C/mL for potassium ion and calcium ion, respectively. Further support for this notion, that charge per unit volume plays the dominant role in the release rate, is demonstrated by calculation of Pearson correlation coefficients for the effect of the independent variables; TEGDA mol %, ion charge density, and charge per unit volume, on the dependent parameters,  $D_{\text{eff}}$  and  $n$ , of the Korsmeyer-Peppas transport model, Table 6. Finally, the First-Order model exhibited a high correlation to the experimental data. This indicates the release profile is dependent on the concentration, which is proportional to charge per unit volume.

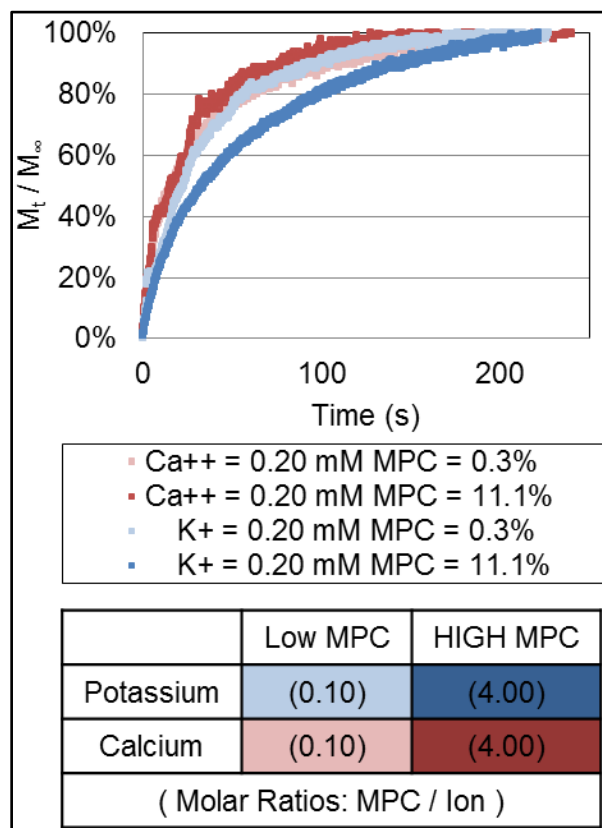
**Table 6.** Pearson correlation coefficients for the effect of dependent variables on independent parameters;  $D_{\text{eff}}$  and  $n$ ; in the Korsmeyer-Peppas transport model.

Parameter	$D_{\text{eff}}$	$n$
TEGDA mol %	0.40	0.25
Ion charge density	0.68	0.92
Charge per unit volume	-0.68	-0.92

The Pearson correlation coefficients for charge per unit volume are negative for both parameters and have the largest absolute value indicating that charge per unit volume is the dominant independent variable in the system and has a negative correlation to the dependent variables.

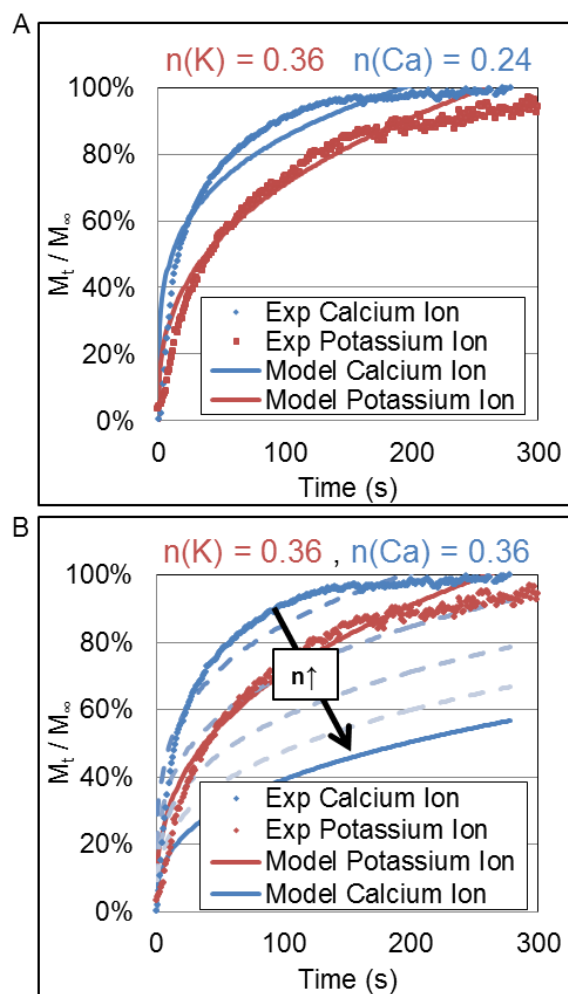
To investigate this further, we measured the potassium ion and calcium ion release profiles from hydrogel microforms that contained the same concentration of potassium ion and calcium ion (0.20 mM) at two separate molar concentrations of MPC within the hydrogel feedstock (0.3 and 11.1 mol % MPC) and a fixed cross-linker (TEGDA) concentration within the feedstock (3 mol %). Those release profiles are shown in Figure 5. Again, the calcium ion was released more quickly from the hydrogel when compared to potassium ion. Moreover, the release of both ions is faster at the higher MPC unit composition suggesting that the presence of the MPC influences the microstructure of the hydrogel or its electromigration characteristics.

**Figure 5.** Release profiles of the potassium ion (**blue** and **light Blue**) and calcium ion (**red** and **orange**) from hydrogel with varying composition of MPC (0.3 and 11.1 mol %). The cross-linking density was fixed by 3.0 mol % of TEGDA and fixed loading of ions within the hydrogel microform (0.2 mM).



Currently, it is unclear which electrostatic interaction is causing the observed effect; however, it is proposed that electromigration is the likely candidate. It is observed that divalent calcium ion releases more rapidly than monovalent potassium ion. If binding effects and/or virtual crosslinking played a dominant role in the release, then it is expected that calcium ion would be released more slowly than potassium as virtual crosslinks could occur and calcium ion would likely form more ionic bonds than potassium due to its 2+ valence. Conversely, since calcium ion had a charge per unit volume that was approximately 20× that of potassium and it released more rapidly, the release is most likely dominated by electromigration effects due to charge density gradients across the hydrogel–buffer interface. To confirm and demonstrate this effect, a simulation was conducted wherein the Korsmeyer-Peppas transport model was parameterized with the extracted values of  $D_{\text{eff}}$  and  $n$ . Figure 6 shows influence of the  $n$  parameter on the release profiles of calcium ions and potassium ions. Figure 6A shows the average release profile and the fit of the Korsmeyer-Peppas equation using the  $D_{\text{eff}}$  and  $n$  values derived from the best fit of the actual data. Figure 6B shows the quality of that fit as the value  $n$  is increased from 0.24 to 0.36; a value corresponding to that obtained for potassium ions. Clearly, a larger value of  $n$  for calcium ions that is of the same magnitude as that of potassium ions would cause its release rate to be slower than that of potassium ions. Thus, despite having quite similar charge densities, the divalency of  $\text{Ca}^{++}$  produces a faster release rate.

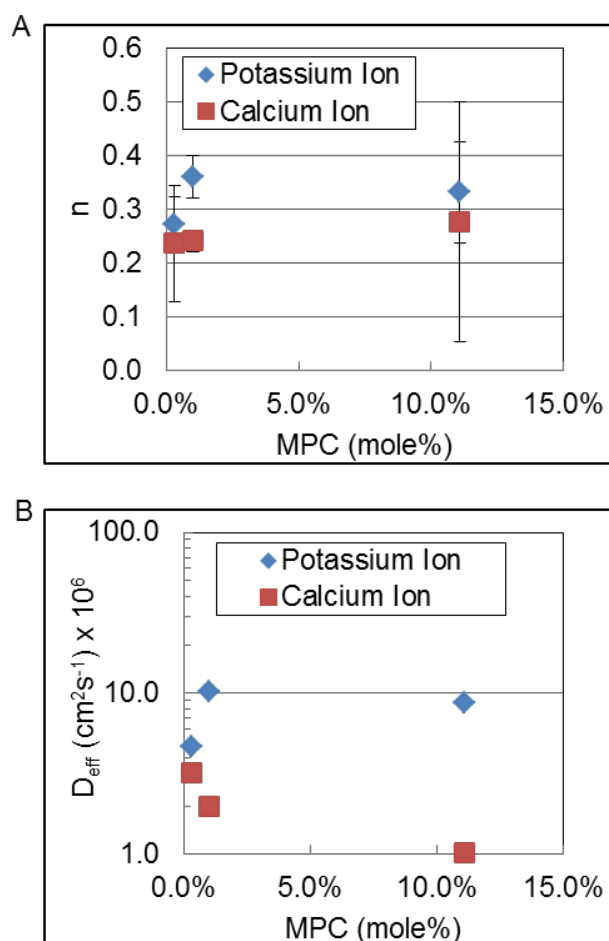
**Figure 6.** Release profiles of the potassium ion (**blue**) and calcium ion (**red**) from hydrogel with varying composition of MPC (0.3 and 11.1 mol %). The cross-linking density was fixed by 3.0 mol % of TEGDA and a fixed loading of ions within the hydrogel microform (0.2 mM). (A) A fit of the K-P model to experimental data for values of  $n$  determined experimentally; and (B) Downward shifts in the release profile for potassium ion for increasing values of  $n$  and the predicted release profile for potassium ion if  $n = 0.36$ , same as calcium ion.



Finally, to address the possible influence of MPC content on the release we studied potassium ion and calcium ion release at three different MPC mole percentages, 0.3, 1.0 and 11.1 mol %. Figure 7 shows the trends in the magnitude of the  $n$  parameter and the effective diffusion coefficient,  $D_{\text{eff}}$  ( $\text{cm}^2 \cdot \text{s}^{-1}$ ), of potassium ions and calcium ions as a function of MPC content of the hydrogel. The  $n$ -parameter remains essentially constant for each type of ion. However, the apparent diffusion coefficient increases for the potassium ion while it decreases for the calcium ion confirming that there is interaction of the divalent calcium ion with the PC moieties of the hydrogel.

Further investigation into electromigratory transport effects in hydrogels is ongoing as it is of interest since the fundamental understanding of this phenomenon will be important for the development of many biotechnical applications.

**Figure 7.** Trends in the magnitude of the  $n$  parameter (A) and the effective diffusion coefficient,  $D_{\text{eff}}$  ( $\text{cm}^2 \cdot \text{s}^{-1}$ ); and (B) of potassium and calcium ions as a function of MPC content of the hydrogel.



## 5. Conclusions

Based on these findings, we are unable to affect the release profiles of potassium and calcium ions by changing crosslink density using these experimental methods. Results were fitted to the Korsmeyer-Peppas model because it had the strongest correlation to the measured data ( $R^2 > 0.9$ ). Resulting diffusion coefficients were found to be  $2.6 \times 10^{-6}$  and  $11.2 \times 10^{-6}$   $\text{cm}^2/\text{s}$  for calcium ion and potassium ion, respectively. These values correspond quite closely with those found in the literature for ion diffusion through buffer;  $2.3 \times 10^{-6}$  and  $19.2 \times 10^{-6}$   $\text{cm}^2/\text{s}$  for calcium ion [14] and potassium ion [34], respectively. The diffusion exponents of calcium ion and potassium ions ( $n_{\text{Ca}^{++}} = 0.24$ ,  $n_{\text{K}^+} = 0.36$ ) indicate that the mechanism of diffusion is non-Fickian ( $n < 0.5$ ). Based on Pearson correlation coefficients and release profiles it is likely that electromigratory effects are contributing to the non-Fickian diffusion mechanism. Migratory release models should be investigated further. Additional studies should include determining the existence of a dependence on ion release to the ratio of MPC unit composition to ion concentration and pH. It could be possible that saturated or unsaturated conditions could vary ion release.

## Acknowledgments

This work was supported by the US Department of Defense (DoDPRMRP) grant PR023081/DAMD17-03-1-0172, by the Calhoun Honors College at Clemson University, by the Consortium of the Clemson University Center for Bioelectronics, Biosensors and Biochips (C3B) and by ABTECH Scientific, Inc.

## Conflicts of Interest

The authors declare no conflict of interest.

## References

1. Karunwi, O.; Wilson, A.N.; Kotanen, C.; Guiseppi-Elie, A. Engineering the abio-bio interface to enable more than moore in functional bioelectronics. *J. Electrochem. Soc.* **2013**, *160*, B60–B65.
2. Peppas, N.; Bures, P.; Leobandung, W.; Ichikawa, H. Hydrogels in pharmaceutical formulations. *Eur. J. Pharm. Biopharm.* **2000**, *50*, 27–46.
3. Wilson, A.N.; Salas, R.; Guiseppi-Elie, A. Bioactive hydrogels demonstrate mediated release of a chromophore by chymotrypsin. *J. Control. Release* **2012**, *160*, 41–47.
4. Slaughter, B.V.; Khurshid, S.S.; Fisher, O.Z.; Khademhosseini, A.; Peppas, N.A. Hydrogels in regenerative medicine. *Adv. Mater.* **2009**, *21*, 3307–3329.
5. Guiseppi-Elie, A.; Dong, C.; Dinu, C.Z. Crosslink density of a biomimetic poly(HEMA)-based hydrogel influences growth and proliferation of attachment dependent RMS 13 cells. *J. Mater. Chem.* **2012**, *22*, 19529–19539.
6. Park, J.H.; Bae, Y.H. Hydrogels based on poly(ethylene oxide) and poly(tetramethylene oxide) or poly(dimethyl siloxane): Synthesis, characterization, *in vitro* protein adsorption and platelet adhesion. *Biomaterials* **2002**, *23*, 1797–1808.
7. Wilson, A.N.; Guiseppi-Elie, A. Bioresponsive hydrogels. *Adv. Healthc. Mater.* **2013**, *2*, 520–532.
8. Gawel, K.; Barriet, D.; Sletmoen, M.; Stokke, B.T. Responsive hydrogels for label-free signal transduction within biosensors. *Sensors* **2010**, *10*, 4381–4409.
9. Ganji, F.; Vasheghani-Farahani, S.; Vasheghani-Farahani, E. Theoretical description of hydrogel swelling: A review. *Iran. Polym. J.* **2010**, *19*, 375–398.
10. Kotanen, C.N.; Wilson, A.N.; Dong, C.; Dinu, C.-Z.; Justin, G.A.; Guiseppi-Elie, A. The effect of the physicochemical properties of bioactive electroconductive hydrogels on the growth and proliferation of attachment dependent cells. *Biomaterials* **2013**, *34*, 6318–6327.
11. Nakamura, S.; Matsumoto, T.; Sasaki, J.-I.; Egusa, H.; Lee, K.Y.; Nakano, T.; Sohmura, T.; Nakahira, A. Effect of calcium ion concentrations on osteogenic differentiation and hematopoietic stem cell niche-related protein expression in osteoblasts. *Tissue Eng. A* **2010**, *16*, 2467–2473.
12. Guiseppi-Elie, A. Electroconductive hydrogels: Synthesis, characterization and biomedical applications. *Biomaterials* **2010**, *31*, 2701–2716.
13. Peng, C.-C.; Chauhan, A. Ion transport in silicone hydrogel contact lenses. *J. Membr. Sci.* **2012**, *399*, 95–105.

14. Kotanen, C.N.; Wilson, A.N.; Wilson, A.M.; Ishihara, K.; Guiseppi-Elie, A. Biomimetic hydrogels gate transport of calcium ions across cell culture inserts. *Biomed. Microdevices* **2012**, *14*, 549–558.
15. Boztas, A.O.; Guiseppi-Elie, A. Immobilization and release of the redox mediator ferrocene monocarboxylic acid from within cross-linked p(HEMA-co-PEGMA-co-HMMA) hydrogels. *Biomacromolecules* **2009**, *10*, 2135–2143.
16. Tong, J.; Anderson, J.L. Partitioning and diffusion of proteins and linear polymers in polyacrylamide gels. *Biophys. J.* **1996**, *70*, 1505–1513.
17. Geise, G.M.; Freeman, B.D.; Paul, D.R. Sodium chloride diffusion in sulfonated polymers for membrane applications. *J. Membr. Sci.* **2013**, *427*, 186–196.
18. Omidian, H.; Park, K. Introduction to Hydrogels. In *Biomedical Applications of Hydrogels Handbook*; Springer: New York, NY, USA, 2010; pp. 1–16.
19. Flory, P.J.; Rehner, J., Jr. Statistical mechanics of cross-linked polymer networks II. Swelling. *J. Chem. Phys.* **1943**, *11*, 521–526.
20. Peppas, N.A.; Merrill, E.W. Crosslinked poly(vinyl alcohol) hydrogels as swollen elastic networks. *J. Appl. Polym. Sci.* **1977**, *21*, 1763–1770.
21. De, S.K.; Aluru, N.; Johnson, B.; Crone, W.; Beebe, D.J.; Moore, J. Equilibrium swelling and kinetics of pH-responsive hydrogels: Models, experiments, and simulations. *Microelectromech. Syst. J.* **2002**, *11*, 544–555.
22. Mafe, S.; Manzanares, J.A.; Reiss, H. Donnan phenomena in membranes with charge due to ion adsorption. Effects of the interaction between adsorbed charged groups. *J. Chem. Phys.* **1993**, *98*, 2325–2331.
23. Abraham, S.; Brahim, S.; Ishihara, K.; Guiseppi-Elie, A. Molecularly engineered p(HEMA)-based hydrogels for implant biochip biocompatibility. *Biomaterials* **2005**, *26*, 4767–4778.
24. Lee, W.-F.; Lin, Y.-H. Swelling behavior and drug release of NIPAAm/PEGMEA copolymeric hydrogels with different crosslinkers. *J. Mater. Sci.* **2006**, *41*, 7333–7340.
25. Dash, S.; Murthy, P.N.; Nath, L.; Chowdhury, P. Kinetic modeling on drug release from controlled drug delivery systems. *Acta Poloniae Pharm.* **2010**, *67*, 217–223.
26. Ishihara, K.; Ueda, T.; Nakabayashi, N. Preparation of phospholipid polymers and their properties as polymer hydrogel membranes. *Polym. J.* **1990**, *22*, 355–360.
27. Higuchi, T. Mechanism of sustained-action medication. Theoretical analysis of rate of release of solid drugs dispersed in solid matrices. *J. Pharm. Sci.* **1963**, *52*, 1145–1149.
28. Hixson, A.; Crowell, J. Dependence of reaction velocity upon surface and agitation. *Ind. Eng. Chem.* **1931**, *23*, 923–931.
29. Korsmeyer, R.W.; Gurny, R.; Doelker, E.; Buri, P.; Peppas, N.A. Mechanisms of solute release from porous hydrophilic polymers. *Int. J. Pharm.* **1983**, *15*, 25–35.
30. Carr, L.R.; Xue, H.; Jiang, S. Functionalizable and nonfouling zwitterionic carboxybetaine hydrogels with a carboxybetaine dimethacrylate crosslinker. *Biomaterials* **2011**, *32*, 961–968.
31. Hamilton, C.J.; Murphy, S.M.; Atherton, N.D.; Tighe, B.J. Synthetic hydrogels: 4. The permeability of poly(2-hydroxyethyl methacrylate) to cations—An overview of solute—Water interactions and transport processes. *Polymer* **1988**, *29*, 1879–1886.

32. Kikuchi, M.; Terayama, Y.; Ishikawa, T.; Hoshino, T.; Kobayashi, M.; Ogawa, H.; Masunaga, H.; Koike, J.-I.; Horigome, M.; Ishihara, K.; *et al.* Chain dimension of polyampholytes in solution and immobilized brush states. *Polym. J.* **2012**, *44*, 121–130.
33. Matsuda, Y.; Kobayashi, M.; Annaka, M.; Ishihara, K.; Takahara, A. Dimension of poly(2-methacryloyloxyethyl phosphorylcholine) in aqueous solutions with various ionic strength. *Chem. Lett.* **2006**, *35*, 1310–1311.
34. Donini, A.; O'Donnell, M.J. Analysis of Na<sup>+</sup>, Cl<sup>-</sup>, K<sup>+</sup>, H<sup>+</sup> and NH<sup>4+</sup> concentration gradients adjacent to the surface of anal papillae of the mosquito *Aedes aegypti*: Application of self-referencing ion-selective microelectrodes. *J. Exp. Biol.* **2005**, *208*, 603–610.

© 2013 by the authors; licensee MDPI, Basel, Switzerland. This article is an open access article distributed under the terms and conditions of the Creative Commons Attribution license (<http://creativecommons.org/licenses/by/3.0/>).